

Detection of Activated, TIMP-free MMPs

MMP inhibitor-tethered resins provide a method for detection of activated MMPs in tissues [1]. These measurements will help to elucidate in situ mechanisms of MMP activation, further our understanding of the tumor microenvironment, and facilitate development of MMP-inhibitor therapy.

Matrix metalloproteinases (MMPs) are a large family of zinc-dependent endoproteases that have been implicated in many physiologic and pathologic processes. This field of scientific interest emerged in 1962 from the discovery of interstitial collagenase (later renamed MMP-1) as a result of experiments designed to explain collagen remodeling during tadpole metamorphosis [2]. Basic MMP research for the next three decades focused on the activation of MMPs and the ensuing degradation of extracellular matrix components (collagens, laminin, fibronectin, etc.) [3]. Activation of MMPs is achieved by removal of the N-terminal prosequence of ~80 amino acids by a two-step process. The initial cleavage occurs in the accessible “bait” region located between the first and second α helix in the propeptide domain. This cleavage destabilizes the interaction of the propeptide with the catalytic domain, leading to a final cleavage often occurring as a bimolecular, autolytic event. Clinical interest in the role of MMPs in physiologic and pathologic processes gradually mushroomed, and now exceeds more than 1000 publications per year.

High tissue levels of MMP-1, -2, -3, -7, -8, -9, -11, -13, and -14 (MT1-MMP) have been demonstrated in many types of human cancer; correlation with poor clinical outcome has been reported. Not only are MMPs increased in the tumor cells, but they are also increased in stromal (fibroblasts, endothelial cells) and inflammatory cells within tumors. The contribution of stromal MMPs to tumor progression is hotly debated. Increased tissue levels of MMPs have also been identified in inflammatory diseases including arthritis, colitis, periodontitis, atherosclerosis, and cerebrovascular disease. (Interested readers are referred to relevant review articles [4–9].)

In vivo activity of MMPs is rigidly controlled at several levels. These enzymes are usually expressed in low amounts, and their transcription is tightly regulated [10]. MMP-2 is the exception to the general rule and is constitutively produced and activated on the cell surface by membrane type 1-MMP (Figure 1; MT1-MMP). Activation of other secreted MMPs also occurs by removal of the prodomain by proteolytic or nonproteolytic mechanisms that are not well understood. MMPs that contain a furin-like recognition domain in their propeptide (MMP-11, MMP-28, and MT 1-MMP) are activated intracellularly. Once activated, MMPs are further regulated by endogenous inhibitors, autodegradation, and

selective endocytosis [11]. In normal physiology, high extracellular concentrations of tissue inhibitors of metalloproteinases (TIMP-1, -2, -3, and -4) and α 2-macroglobulin (α 2M) oppose random MMP activation. Most cells secrete both MMPs and TIMPs, as well as activators of MMPs. Hence, the function of activated MMPs tends to be limited to short bursts of time in the pericellular microenvironment. MMPs bound to the cell surface are partially protected from TIMP inhibition.

The simplicity of thinking about MMPs solely as extracellular matrix degrading enzymes and TIMPs solely as inhibitors of these processes has recently been eroded by the recognition of numerous other important roles for these proteins. Extracellular matrix-localized growth factors, e.g., basic fibroblast growth factor (β FGF), transforming growth factor β (TGF- β), as well as cell surface bound precursors of growth factors, are released as functional molecules following cleavage by activated MMPs. Growth factor receptors, such as fibroblast growth factor receptor 1, interleukin-2 receptor α , and integrins can be cleaved from the cell surface by MMPs. Other examples of substrates cleaved by MMPs include proteins involved in apoptosis, angiogenesis, cell migration, and evasion of immune surveillance [4–9]. Exposure of cryptic sites that contain signaling information for responsive cells is another common theme of MMPs [12]. Through these pathways, MMP cleavage would appear to facilitate cancer invasion and metastasis; however, cleavage of some substrates can interfere with cancer dissemination, i.e., MMP-induced cleavage of plasminogen results in generation of angiostatin, an inhibitor of tumor angiogenesis [4–9]. The major difference between physiologic processes and dissemination of cancer cells seems to be one of regulation.

MMP expression profiles have been reported to be useful in explicating various disease processes [13]. Yet, the critical question vexing scientists for the past decade is: Does the presence of high tumor concentrations of MMPs indicate that they have a causative role in cancer progression/dissemination? As repeatedly emphasized, correlation does not necessarily mean causation [14]. However, measurement of MMPs in tissues is not trivial. A practical problem in quantifying levels of MMPs in clinical samples relates to genetic differences in MMP expression. Additionally, specific MMPs have different functions depending on the stage of cancer and the local milieu of the cancer cells.

Emphasis has been placed on the importance of active rather than total MMP levels in tumors [15]. However, technical problems in the identification of activated MMPs in tissues have limited this assessment. The fact that activated MMPs have not been detected in the blood of cancer patients suggests that endogenous inhibitors rapidly bind and inactivate mature proteases in tissues and blood [7]. The high ratio of MMPs to TIMPs in cancer tissue specimens has been proposed to reflect dominant proteolytic activity and has been correlated with poor prognosis [3–7].

Gelatin substrate zymography has been used widely as a sensitive, inexpensive technique to detect both

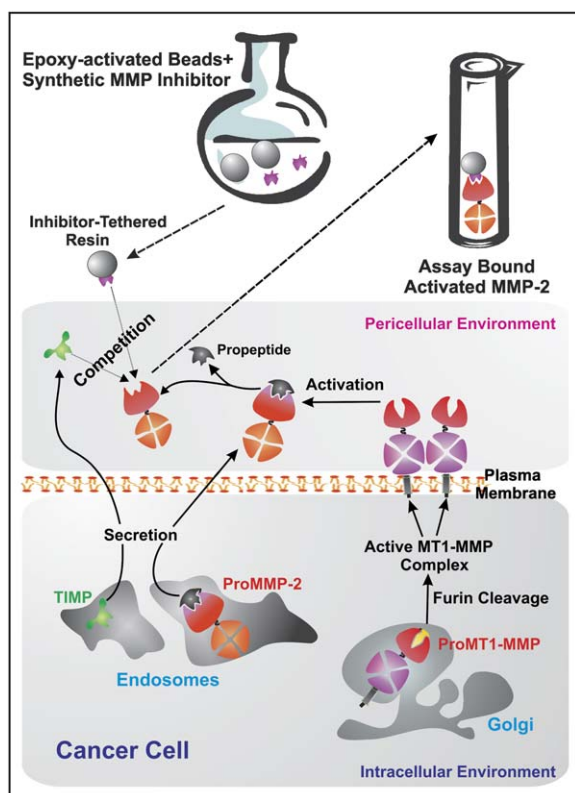


Figure 1. Cartoon Describing the Competition between Exogenous MMP Inhibitor-Tethered Resin Binding and Endogenous TIMP Binding of Activated MMP-2 in the Extracellular Space

Following propeptide cleavage, the catalytic site of MMP-2 is exposed and capable of binding to inhibitors. For simplicity, the triplex formed on the cell surface consisting of MT1-MMP, TIMP-2, and proMMP-2 leading to generation of activated MMP-2 is omitted.

MMP-2 and -9 and to distinguish between latent and activated proteases. However, this technique does not permit distinction between free MMP and active protease bound to TIMP or $\alpha 2M$. Enzyme-linked immunosorbent assays are reliable, sensitive, and available commercially, but do not distinguish between active and latent MMPs [7]. DNA microarray, real-time RT-PCR, and proteomic approaches have more recently been proposed as techniques to target the profiling of proteases in cancer [16]. These technologies are limited by not addressing functional activity of MMPs.

In this issue of *Chemistry & Biology*, Heseck et al. [1] report the comprehensive design and characterization of a resin-immobilized potent broad-spectrum synthetic MMP inhibitor for the selective detection of active forms of MMPs in experimental samples. Only the free active MMPs, and not the zymogens or MMP/TIMP complexes, were bound specifically to the resin. On examination of human tissue, active (free) MMP-2 and MMP-14 were detected in cancerous, but not in benign, human tissue extracts. The authors propose that the identification of the active MMP profile for individual cancer types will help to target specific MMPs on an individual basis, hence encouraging future development of specific/selective inhibitory drugs for treatment of

cancer. Based on the data presented, it would appear that a fluorescent immobilized resin approach might also be applicable for in situ detection of active MMPs in living tissue. This type of approach has the potential to illuminate the mystery of pericellular protease activation.

As an example of tissue specimens readily accessible for future study, neutrophils and macrophages have high constitutive levels of MMPs and other proteases, which are released at sites of tissue injury and repair. These inflammatory cells are prominently displayed in tumor stroma. Detection of activated MMP-9 following degranulation of neutrophils provides a model for how the currently disclosed technology may be useful in expanding our understanding of the pathophysiology of MMPs.

The type of translational research presented in Heseck et al. is sorely needed to reinvigorate pharmaceutical industry interest in developing specific MMP inhibitors for treatment of cancer and inflammatory diseases. The authors wisely caution that a variety of factors, including tissue extraction procedure and sample storage, will affect detection of active MMPs in tissue samples. However, these technical problems may limit widespread utilization of metalloproteinase inhibitor-tethered resin examination of clinical tissues for diagnosis, staging, and prognosis of cancer. One alternative is the development of techniques to identify the cleavage products released following activation of latent MMPs [7]. These “footprints” remaining after MMP activation include the N-terminal and C-terminal activation products released from MMPs themselves [17] or cleaved from extracellular matrix proteins.

Stanley Zucker^{1,2} and Jian Cao^{1,2}

¹ Department of Research and Medicine

VA Medical Center

Northport, New York 11768

² School of Medicine

Stony Brook University

Stony Brook, New York 11794

Selected Reading

1. Heseck, D., Toth, M., Meroueh, S.O., Brown, S., Zhao, H., Sakr, W., Fridman, R., and Mobashery, S. (2006). *Chem. Biol.* 13, this issue, 379–386.
2. Gross, J., and Lapiere, C.M. (1962). *Proc. Natl. Acad. Sci. USA* 48, 1014–1022.
3. Birkedal-Hansen, H., Moore, W.G.I., Bodden, M.K., Windsor, L.J., Birkedal-Hansen, B., DeCarlo, A., and Engler, J.A. (1993). *Crit. Rev. Oral Biol. Med.* 42, 197–250.
4. McCawley, L.J., and Matrisian, L.M. (2000). *Mol. Med. Today* 6, 149–156.
5. Egeblad, M., and Werb, Z. (2002). *Nat. Rev. Cancer* 2, 163–176.
6. Overall, C.M., and Lopez-Otin, C. (2002). *Nat. Rev. Cancer* 2, 657–672.
7. Zucker, S., Doshi, K., and Cao, J. (2004). *Adv. Clin. Chem.* 38, 37–85.
8. Stamenkovic, I. (2000). *Cancer Biol.* 10, 415–433.
9. Fingleton, B. (2006). *Front. Biosci.* 11, 479–491.
10. Nagase, H., and Woessner, F. (1999). *J. Biol. Chem.* 274, 21491–21494.
11. Yang, Z., Strickland, D.K., and Bornstein, P. (2001). *J. Biol. Chem.* 276, 8403–8408.

12. Xu, J., Rodriguez, D., Petittler, E., Kim, J.J., Hangai, M., Yuen, S.M., Davis, G.E., and Brooks, P.C. (2001). *J. Cell Biol.* **154** (5), 1069–1079.
13. Ye, S., Eriksson, P., Hamsten, A., Kurkinin, M., Humphries, S.E., and Henney, A.M. (1996). *J. Biol. Chem.* **271**, 13055–13060.
14. Stetler-Stevenson, W., Hewitt, R.E., and Corcoran, M.L. (1996). *Semin. Cancer Biol.* **7**, 147–154.
15. Brown, P.D., Bloxidge, R.E., Anderson, E., and Howell, A. (1993). *Clin. Exp. Metastasis* **11**, 183–189.
16. Overall, C.M., Tam, E.M., Kappelhoff, R., Conner, A., Ewart, T., Morrison, C.J., Puente, X.S., Lopez-Otin, C., and Seth, A. (2004). *Biol. Chem.* **385**, 493–504.
17. Osenkowski, P., Toth, M., and Fridman, R. (2004). *J. Cell. Physiol.* **200**, 2–10.

New Images Evoke FAScinating Questions

Two recent papers in *Science* reported the X-ray structures of the large, organizationally distinct animal and fungal fatty acid synthases at 5 Å. These new structural insights have unexpected implications for enzyme function for the other “iterative” and “assembly line” megasynthases.

Five years ago, we saw the bacterial ribosome at 5 Å resolution [1–6]. Now, two landmark papers appearing recently in *Science* present the first views of two fatty acid synthases (FASs) at similar resolution, another important cellular macromolecular machine. Through a complex catalytic mechanism involving decarboxylative condensation, reduction, and dehydration activities, FAS produces long-chain fatty acids from acetyl-CoA and malonyl-CoA units. The protein in mammals is encoded by a single gene, consists of seven catalytic domains, and is functional as a homodimer (α_2). In surprising contrast, analogous domains in fungi are distributed between two subunits, and a giant, structurally distinct $\alpha_6\beta_6$ barrel carries out the corresponding reactions, although it releases its fatty acid product as the CoA ester rather than the free acid as in the case of mammalian FAS.

The breakthrough in the 3D structural elucidation of animal FAS provides new insights and resolves the ongoing controversy over the structure of the enzyme. The original model formulated in the 1980s envisioned the two α -subunits of FAS oriented in an extended antiparallel arrangement in which a noncatalytic central core stabilized the dimeric structure [7]. Stuart Smith and co-workers proposed a revision of this view in accordance with key biochemical findings and EM data highlighting both intra- and interfunctional interactions of the subunits [8, 9]. Although the resolution of the current crystal structure is insufficient to trace the complete backbone of the individual subunits, the authors have fit atomic-resolution structures of homologous individual bacterial proteins into the electron density map of mammalian FAS to reveal the location of most of the functional domains. The model proposed by the authors depicts two coiled subunits oriented head-to-head with paired, centrally located KS domains stabilizing the dimer in

close agreement with the predictions of Smith. The X-shaped model consists of a main body composed of the ER and KS dimers and the pseudodimeric DH pairs, while the monomeric KR and MT domains are located peripherally at the top and bottom of the model, respectively (Figure 1, left). The active sites of the two sets of catalytic domains are oriented facing each of the two lateral clefts in the structure, thus forming two asymmetric reaction chambers. While ambiguities exist in the structure, for example, the key ACP and TE domains cannot be clearly discerned, the crystal structure presents a model that largely accommodates previous biochemical findings.

As with the mammalian enzyme, EM analysis has provided a global view of fungal FAS. While the limits of resolution did not permit localization of individual domains, it did allow general placement of the α and β subunits within the $\alpha_6\beta_6$ barrel [10, 11]. The X-ray structure has now provided a sharper view in which active sites have been approximated within most of the catalytic domains in the enormous 230 × 260 Å cage-like superstructure (Figure 1, right). Three sets of active sites face inward within two identical reaction chambers. Each chamber contains openings as large as 25 Å, permitting substrates and products to passively diffuse in and out as their CoA esters. The structure determined at lower resolution (8 Å) identified a potential attachment region for the ACP located in the interior and accessible for interactions among the domains of multiple subunits, which agrees well with earlier biochemical studies [12].

Interestingly, the order of catalytic domains in animal FAS parallels the bacterial type I modular, or “assembly line,” polyketide synthases (PKSs) responsible for the biosynthesis of a wide variety of macrolide and polyether natural products as, for example, erythromycin [13, 14]. The type I modular PKS model of intertwined dimeric helices deduced by Peter Leadlay and Jim Staunton has proved prescient in guiding thoughts not only about modular PKSs, but also in unifying revision of the long-held view of mammalian FAS head-to-tail dimerization [14, 15]. Nonribosomal peptide synthetases (NRPSs), a parallel universe of giant, modular enzymes that make, for example, the precursors of penicillin and vancomycin, are organized and function in an analogous manner [16, 17]. The synthetic potential of PKSs and NRPSs is adroitly combined in Nature to synthesize metabolites like epothilone and rapamycin [18].